International Journal of Engineering Research & Technology (IJERT)
ISSN: 2278-0181
Vol. 14, Issue 06, ACSCON - 2026

Solar Powered Electric Vehicle With A Battery Swapping System

Prof. Chaithanya S
Department of Electronics and Communication Engineering
Rajarajeswari college of Engineering
Bangalore, India
chaithanya06@gmail.com

Balaji T
Department of Electronics and Communication Engineering
Rajarajeswari college of Engineering
Bangalore,India
karthikbalaji37@gmail.com

Harsha G N
Department of Electronics and Communication Engineering
Rajarajeswari college of Engineering Bangalore,India
harshanharsha141@gmail.com

K Kiran N Swamy
Department of Electronics and Communication Engineering
Rajarajeswari college of Engineering
Bangalore,India
kkirannswamy11@gmail.com

Ajay K N
Department of Electronics and Communication Engineering
Rajarajeswari college of Engineering
Bangalore,India
ajayathish05@gmail.com

***Abstract*— The global transition toward sustainable mobility has accelerated the adoption of Electric Vehicles (EVs); however, challenges regarding limited range, prolonged charging times, and reliance on non-renewable grid power persist. To address these limitations, this paper presents the design and implementation of a solar-powered electric vehicle integrated with an intelligent dual-battery swapping system. The proposed architecture utilizes a twin-battery configuration that enables simultaneous charging and discharging—powering the vehicle with one battery bank while the standby bank replenishes energy via an 80 W onboard solar photovoltaic (PV) system. Centralized control is achieved using an ESP32 microcontroller, which governs the automated swapping logic based on real-time State of Charge (SOC) and voltage monitoring. Additionally, an Internet of Things (IoT) telemetry system is implemented for remote monitoring of battery health and vehicle diagnostics. Experimental results demonstrate that the system successfully executes battery swapping within 800 ms to 1.1 seconds, ensuring uninterrupted vehicle operation. This approach effectively mitigates range anxiety and reduces dependency on external charging infrastructure, offering a viable solution for sustainable, self-sufficient EV operation.**

Keywords*— *Electric Vehicle (EV), Solar Photovoltaic (PV), Battery Swapping System, Dual Battery Management, ESP32, Internet of Things (IoT)

I. INTRODUCTION

A significant change in transportation is being driven by the global mandate to reduce greenhouse gas emissions, which makes Electric Vehicles (EVs) essential to sustainable mobility. However, reliance on grid-based charging from non-renewable sources sometimes negates the environmental benefits of EVs. To build a genuinely sustainable ecosystem, solar photovoltaic (PV) power must be directly integrated with electric vehicle (EV) systems. Power electronics and advanced Battery Management Systems (BMS) have improved efficiency, but persistent problems including delayed charging, limited range, and the inherent unpredictability of solar power still persist.Because conventional charging is constrained by unidirectional power flow and single-battery arrangements, it results in imbalanced loads, extended charging periods, and rapid cell degradation. These constraints substantially diminish reliability. Single-battery designs and conventional methods must be abandoned if electric vehicles are to be actually ecologically beneficial.

A significant architectural answer to these fundamental limitations is provided by the twin battery splitting concept, a promising paradigm that divides the primary energy storage into two connected batteries. Both independent and simultaneous charging and discharging are possible with this configuration. For instance, the motor can be powered by one bank while the other is charged via regenerative braking or solar PV. In addition to improving energy continuity and utilization and simplifying the process of regulating charge levels, this method significantly extends operational lifespan and reduces stress on individual cells.The twin battery design, which is backed by advanced converter topologies with bidirectional energy flow and astute switching devices, allows power control based on driving and environmental conditions. This comprehensive approach integrates renewable energy sources, effective battery splitting, a package that brings together renewable energy, smart battery management, and flexible power control. Here's the thing: while there's been lots of research on solar-powered EVs, we're still missing a key piece. Most current systems use static charging methods that don't adapt to real driving situations. They lack the flexibility to optimize power on the fly. That's exactly what our research aims to fix.

We want to create a solar EV system that can generate its own electricity, reduce reliance on charging stations, and be more reliable overall. We're focusing on four main areas: building an efficient dual battery system, creating low-loss power transfer technology, integrating solar panels for better range, and developing smart control software to keep everything balanced. This research brings some really important improvements to the table. It makes energy more reliable and helps batteries last longer by smartly managing power flow. It creates a sustainable

International Journal of Engineering Research & Technology (IJERT)
ISSN: 2278-0181
Vol. 14, Issue 06, ACSCON - 2026

system that can power itself, which works not just for electric vehicles but also for storing renewable energy and supporting hybrid power grids. It does this by smoothly combining solar power with a dual battery setup.

.

II. Literature Survey

A. Solar-Powered Electric Vehicles

Solar energy integration in electric vehicles has been extensively researched as a means to extend vehicle range and reduce reliance on grid infrastructure. Studies by [5] demonstrated that solar panels mounted on vehicle surfaces can provide 3-5 kWh of energy per day under optimal conditions, sufficient for 15-25 km of additional range in compact vehicles. However, challenges related to limited surface area, variable solar irradiance, and panel efficiency continue to limit the complete solar autonomy of full-sized vehicles [6].

Research by [7] explored the use of Maximum Power Point Tracking (MPPT) algorithms to optimize solar energy extraction under varying environmental conditions. Their comparative analysis of Perturb and Observe (P&O), Incremental Conductance, and Fuzzy Logic-based MPPT techniques revealed that adaptive algorithms achieve 15-20% higher efficiency compared to conventional PWM charge controllers.

B. Battery Management and Swapping Systems

Battery management systems (BMS) are critical for ensuring safety, longevity, and optimal performance of battery packs in electric vehicles. Comprehensive BMS solutions incorporate state-of-charge (SOC) estimation, state-of-health (SOH) monitoring, cell balancing, and thermal management [8].The concept of battery swapping for electric vehicles was commercialized by companies like Better Place and NIO, demonstrating technical feasibility but facing challenges in standardization and infrastructure investment [9]. Research by [10] compared battery swapping with fast charging, concluding that swapping offers advantages in time efficiency (3-5 minutes vs. 30-60 minutes) but requires significant infrastructure investment and battery standardization.Studies on automated battery swapping mechanisms [11] explored mechanical designs, alignment systems, and safety interlocks. Their prototype achieved swap times of 90 seconds with positioning accuracy within ±5mm, demonstrating the viability of automated systems.

C. IoT-Based Vehicle Monitoring and Control

Internet of Things (IoT) technologies enable remote monitoring, diagnostics, and control of vehicle systems through wireless connectivity. Research by [12] implemented cloud-based monitoring of battery parameters, motor performance, and environmental conditions using ESP8266 microcontrollers with MQTT protocol for data transmission.

Comparative studies of microcontroller platforms for IoT applications [13] evaluated Arduino, ESP32, and Raspberry Pi across parameters including processing power, power consumption, wireless capabilities, and cost. ESP32 emerged as optimal for automotive applications due to its dual-core processor, integrated Wi-Fi/Bluetooth, low power consumption, and adequate GPIO interfaces.

Bluetooth Low Energy (BLE) protocols have been implemented for vehicle control interfaces [14], providing secure, low-latency communication with smartphone applications. Their system achieved command response times of 50-100ms with effective range of 10-15 meters.

D. Safety Systems and Fault Detection

Comprehensive safety mechanisms are essential for autonomous electric vehicle operation. Research by [15] developed multi-layered protection systems incorporating: Overcurrent detection using Hall-effect sensors, thermal monitoring with distributed temperature sensors, voltage monitoring for overvoltage/undervoltage protection, and emergency shutdown protocols with fail-safe mechanisms.

Machine learning approaches for fault detection in electric vehicles [16] demonstrated that neural network classifiers can identify anomalous operating conditions with 95% accuracy, enabling predictive maintenance and preventing catastrophic failures.

E. Motor Control Strategies

Differential drive control for electric vehicles has been extensively studied for achieving precise manoeuvrability. Research by [17] implemented PID control algorithms for individual wheel speed control, achieving accurate trajectory tracking with position error less than 5cm over 10-meter distances.PWM-based speed control for DC motors [18] investigated the relationship between PWM frequency, duty cycle, and motor efficiency. Their findings indicated that frequencies between 10-20 kHz provide optimal trade-offs between switching losses and motor smoothness.

F. Research Gaps

Analysis of existing literature reveals several research gaps:

1. Limited integration of solar energy, battery swapping, and IoT monitoring in a single cohesive system.
2. Insufficient focus on safety mechanisms for automated battery swapping.
3. Lack of comparative analysis between manual and automatic operation modes.
4. Minimal research on low-cost implementations suitable for developing regions.
5. Limited validation of complete systems under diverse environmental conditions.

III. Methodology

A. Design Philosophy and System Architecture

A methodical modular design approach that prioritized scalability, maintainability, and ease of troubleshooting was used in the creation of the solar-powered electric car with intelligent battery swapping and Internet of Things-based monitoring. The central control unit, motor drive system, dual-battery power management, solar charging system, sensor network, and safety monitoring system are the six interconnected subsystems that make up the overall system architecture. Each of these subsystems has distinct interfaces and roles.

The ESP32 microcontroller is used to implement the central control unit, which acts as the hub for coordination and

International Journal of Engineering Research & Technology (IJERT)
ISSN: 2278-0181
Vol. 14, Issue 06, ACSCON - 2026

processing for all subsystems. The requirement for the simultaneous management of several tasks, such as real-time sensor data collecting, motor control signal generation, wireless communication handling, safety monitoring, and user interface management, motivated this architectural choice. The ESP32's dual-core Xtensa LX6 CPU, running at 240 MHz, has enough processing power for real-time control, and its built-in Wi-Fi and Bluetooth capabilities reduce system complexity and expense by doing away with the need for external connection modules. The microcontroller offers sufficient connectivity for a variety of sensors and actuators thanks to its 34 general-purpose input-output pins, 18 analog-to-digital converter channels with 12-bit resolution, and several outputs capable of pulse-width modulation. Additionally, the ESP32 is ideal for battery-powered applications due to its low power consumption features, which include an active current draw of about 160 mA and a deep sleep mode usage of less than 10 µA.

Selection and Integration of Hardware Components Two L298N dual H-bridge driver modules, which can each control two DC motors with a peak capacity of 4 A with suitable heat sinking and a current capacity of up to 2 A per channel during continuous operation, were used to implement motor control. These drivers were chosen because of their simple logic-level control interfaces, sturdy construction with integrated flyback diodes for inductive load protection, and broad operating voltage range of 5 to 35 V. The arrangement of the four DC motors allows for both four-wheel drive operation for maximum torque and two-wheel drive mode for lower power consumption under light load conditions.

The motor's mechanical power output is given by:

$$P_{motor} = T \times \omega \quad (1)$$

where T is the torque produced (N m) and ω is the angular speed (rad/s). The electrical power input to the motor is:

$$P_{elec} = V_m \times I_m \quad (2)$$

The motor efficiency can then be calculated as:

$$\eta_{motor} = \frac{P_{motor}}{P_{elec}} \times 100\% \quad (3)$$

Electromechanical relay modules with 5 V coil voltage and contact ratings of 10 A at 30 V DC were used to switch batteries and manage power distribution. Four relays were assigned: two regulate how Battery 1 and Battery 2 are connected to the load circuit, and two more relays control how solar charging current is routed depending on the battery swap condition. NPN transistors are used in interface circuits to provide appropriate current amplification because relays run on 5 V coils whereas ESP32 outputs are 3.3 V logic levels. A flyback diode was installed on each relay coil to prevent voltage spikes during de-energization.

Cost-effectiveness was given top priority in the sensor selection process while yet ensuring sufficient accuracy. With a sensitivity of 66 mV/A, the ACS712 Hall-effect current sensor (30 A variant) offers isolated measurement. The DHT11 digital temperature and humidity sensor measures temperature between 0 and 50°C with an accuracy of ±2°C and relative humidity between 20 and 80% with an accuracy of ±5%. Precision voltage divider networks with 1% tolerance resistors in 4.3:1 ratios were used to enable battery voltage monitoring, scaling battery voltage to levels appropriate for the ESP32's 3.3 V analog input range.

Power Distribution Network Multiple voltage rails are supported by the power distribution network: a 3.3 V rail for the ESP32 produced by its integrated AMS1117 regulator, a secondary 5 V rail for relay modules and sensors generated by an LM7805 linear regulator (2 A capacity), and a primary 12 V rail for DC motors derived from the active battery. Decoupling capacitors were positioned as follows: 0.1 µF ceramic capacitors at each IC power pin, 100 µF electrolytic capacitors at the battery input, and 100 µF at the LM7805 output.

B. *Solar Power Generation and Energy Calculations*

The power output from the solar photovoltaic panel is given by:

$$P_{solar} = \eta_{pv} \times A_{pv} \times G \quad (4)$$

Where, G is solar irradiance (W/m2), around 1000 W/m² under typical test conditions, A_{pv} is the effective area (m2), andη_{pv} is the solar panel efficiency (usually 15–22%). Appropriate battery capacity and solar panel sizing were determined using power needs estimates. When four-wheel drive is engaged, each of the four DC motors draws about 1.5 A, for a total motor current of 6 A. Relay coils require a total of 280 mA when all four are energised, the ESP32 uses about 250 mA while wireless active, the sensors collectively consume 150 mA, and the display/buzzer uses 100 mA. At 12 V, the whole system peak current need is about 7 A, or 84 W. When a vehicle moves at a speed of v and has a total resistive force of F_r

$$P_{veh} = F_r \times v \quad (5)$$

where resistive force includes rolling and aerodynamic components:

$$F_r = mgf_r + \frac{1}{2}\rho C_d A v^2 \quad (6)$$

with m as vehicle mass (kg), g = 9.81 m/s², f_r as rolling resistance coefficient, ρ as air density (kg/m³), C_d as drag coefficient, and A as frontal area (m²).

Battery capacity was defined as 10 Ah at 12 V nominal, providing 120 Wh energy storage with discharge depth limited to 80% for lead-acid chemistry, based on an anticipated average operating power of 40 W during mixed operation and a targeted runtime of 2-3 hours per battery.

C. *Battery Charging Model*

The energy stored in a battery during charging is:

$$E_{batt} = V_{batt} \times I_{batt} \times t \times \eta_{ch} \quad (7)$$

where V_{batt} is battery voltage (V), I_{batt} is charging current (A), t is charging time (h), and η_{ch} is charging efficiency (typically 0.85-0.95).

When figuring out how big a solar panel you need, you have to consider how much sunlight you get and how efficiently your system charges. For a typical setup running 6 hours a day at 40 watts, you need about 240 watt-hours of energy each day. Things like battery charging efficiency, charge controller performance, and power distribution losses add up to about 30% loss. So your real daily energy need is closer to 312 watt-hours. With an average of 5 peak sun hours per day, the minimum solar panel size would be 312 divided by 5, which is about 62.4 watts. To be safe and have some extra power, an 80 watt polycrystalline solar panel was chosen.

International Journal of Engineering Research & Technology (IJERT)
ISSN: 2278-0181
Vol. 14, Issue 06, ACSCON - 2026

D. System Efficiency Analysis

Overall system efficiency from solar generation to motor drive is:

$$\eta_{sys} = \eta_{pv} \times \eta_{ch} \times \eta_{inv} \times \eta_{motor} \quad (9)$$

where η_{pv} stands for PV panel efficiency, η_{ch} for charging efficiency, η_{inv} for DC-DC converter efficiency, and η_{motor} for motor efficiency. This multiplicative relationship emphasises how crucial it is to maximise total efficiency by optimising each subsystem.

IV. Smart Battery Swapping Methods

A. Estimating the State of Charge

By integrating current over time, one may estimate the battery's state of charge (SOC).

$$SOC(t) = SOC(0) - \frac{1}{C_{batt}} \int_0^t I_{dis}(t)\, dt \quad (10)$$

where $I_{dis}(t)$ is the discharging current at time t (A), C_{batt} is the rated battery capacity (Ah), and SOC(0) is the initial state of charge (%). Although voltage-based SOC estimation is less accurate than coulomb-counting, it doesn't require any extra hardware other than the voltage measurement circuits that are already in place for safetymonitoring.

B. Algorithm for Swapping Control

Through automated management of two battery packs, the clever dual-battery swapping system allows for continuous vehicle operation without charging downtime. Voltage thresholds and SOC conditions are the basis for automatic battery switching:

$$\text{If } V_{batt1} \leq V_{min} \Rightarrow \text{Switch to Battery 2} \quad (11a)$$
$$\text{If } V_{batt2} \leq V_{min} \Rightarrow \text{Switch to Battery 1} \quad (11b)$$

Where, V_{min} is the predetermined cut-off voltage (10.8 V for a 12 V_{batt} to stop deep drain. Hysteresis is used by the swapping decision algorithm to stop fast cycling. In order to provide a sufficient charge disparity, the swap trigger condition requires that the standby charging battery's SOC have increased beyond 80% AND the active battery's SOC has decreased below 20%. In order to prevent oscillation, reverse thresholds are set at 25% and 75%, respectively, forming a 5% hysteresis band.

The meticulously planned steps that make up the swap execution sequence are: (1) pre-swap verification verifies that the standby battery voltage is higher than the minimum safe threshold of 11.5 V; (2) load stabilisation temporarily lowers motor power to 50% duty cycle for 200 ms; (3) relay switching sequence operates in five time-sequenced steps with 50 ms intervals between transitions; (4) post-swap verification measures the new active battery voltage under load; and (5) charging redirection directs solar current to depleted batteries. The range of total swap execution time is 800 ms to 1.1 seconds.

V. Implementation of Safety System and Sensor Integration

A. Methodology for Signal Conditioning

Both digital sensors that communicate using standardized protocols and analog sensors that need signal conditioning are included in the sensor integration approach. Precision voltage divider networks with 1% tolerance metal film resistors are used in battery voltage monitoring circuits. Using 33 kΩ and 10 kΩ resistors, a division ratio of 4.3:1 was determined to monitor 12 V nominal batteries reaching 14.4 V while charging. This ensures that, even at the maximum charging voltage of 14.8 V, the ADC input voltage does not exceed 3.44 V, staying safely inside the 3.3 V maximum rating.

The output voltage produced by the ACS712 current sensor is centered at half supply voltage (2.5 V for a 5 V supply) at zero current, and it varies linearly with current direction. In order to lower noise and greatly increase measurement stability and resolution, several quick samples are collected and averaged. Two exposed parallel conductor traces spaced two millimeters apart are used to assess conductivity in the implementation of a water detection sensor. A 10 kΩ pull-up resistor keeps the digital input at logic HIGH under dry conditions. The resistance decreases to a few kilohms when water fills the gap, drawing the signal closer to the earth. Before verifying water detection, software debouncing requires persistent LOW results over several consecutive samples.

B. Safety Architecture with Multiple Layers.

Defense-in-depth protection against many failure modes is implemented via the safety system:

- **Overcurrent Detection:** Responds quickly to short circuit situations by running every 100 milliseconds. An instantaneous safety mode shift takes place if the measured current is over the 25 A threshold (determined by the wire gauge and component ratings). The 100 ms monitoring cycle limits energy loss by ensuring fault reaction within around 100 ms of commencement.
- **Voltage Monitoring:** Every battery's voltage is checked every one second. When the battery voltage drops below 10.5 V, which indicates a deep discharge, undervoltage detection activates. When the voltage surpasses 14.8 V, overvoltage detection activates, suggesting a potential charge controller malfunction.
- **Thermal Protection:** Graduated reaction with several thresholds for thermal protection. Automatic cooling fan activation occurs when the warning threshold reaches 45°C. At 60°C, the critical threshold sets off safety mode, which disconnects the batteries and stops all motor activity. Hysteresis for fan deactivation is provided by a lower threshold at 35°C.
- **Water Intrusion Detection:** Water bridging conductors are detected by sensors placed in susceptible areas. Instant safety mode activation disconnects all power upon verified detection, and alerts are transmitted via Bluetooth, audio, and visual channels.

Fail-safe shutdown is implemented by the safety mode execution sequence: all motor driver enable pins are set to LOW, instantly stopping motors; all relays are de-energized,

International Journal of Engineering Research & Technology (IJERT)
ISSN: 2278-0181
Vol. 14, Issue 06, ACSCON - 2026

disconnecting batteries from loads and charging sources; an LCD display displays specific fault information; a Bluetooth notification is sent; and a buzzer is continuously activated. Crucially, safety mode prevents automatic restart by being latched and remaining in place even after the fault clears. Only intentional operator intervention with a certain reset command causes the latch to clear, guaranteeing that errors are recognized and looked into prior to restart.

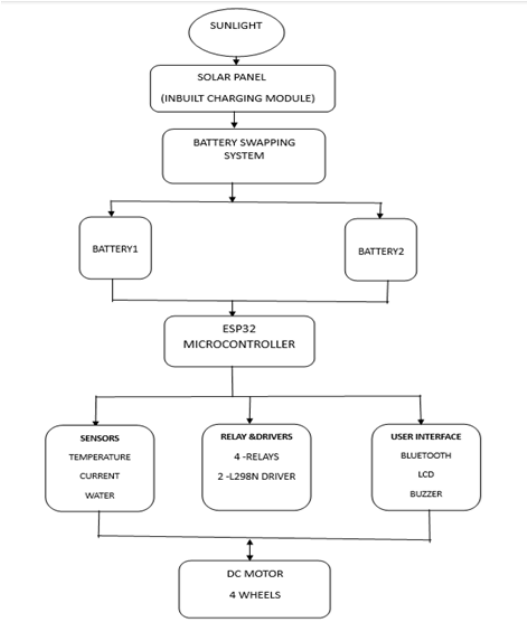

Fig 1. Block diagram

C. *Prototype Assembly*

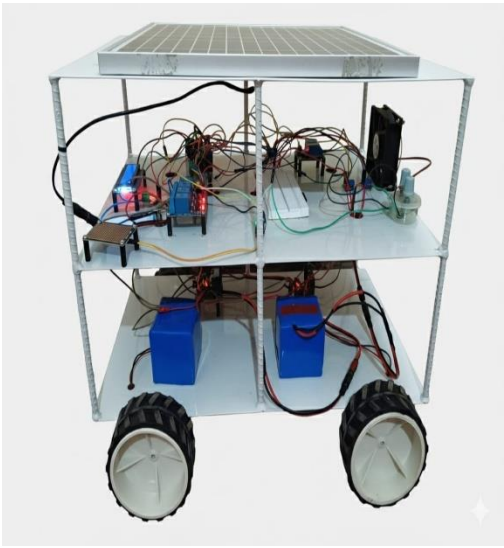

Fig. 2. Hardware implementation of the prototype.

The complete hardware implementation of the proposed system is illustrated in Fig. 2. The prototype integrates the central control unit, utilizing the ESP32 microcontroller, with the power distribution network and the dual-battery storage system. The mechanical chassis supports the 80 W polycrystalline solar panel mounted on the top surface to maximize solar irradiance exposure. Beneath the panel, the electronic control compartment houses the L298N driver modules and the relay bank, which manages the switching logic between the active and standby batteries. The current and voltage sensors are embedded within the wiring harness to provide real-time telemetry to the IoT dashboard, ensuring continuous monitoring of the vehicle's state of charge and operational health.

VI. RESULTS

A. *Solar Charging Characteristics*

Different levels of sun irradiation were used to evaluate the solar charging subsystem. When the irradiation surpassed 200 W/m², the 80 W polycrystalline solar panel successfully started charging. The methodology's three-stage charging profile was followed by the system. The current didn't change during the bulk charging phase until the battery voltage hit the 14.4 V absorption threshold. After the current fell below 0.5 A, the system entered the float phase at 13.6 V. Under peak solar conditions, the average time needed to fully charge the 10 Ah battery from a 20% SOC was found to be roughly 5 hours, confirming the estimated energy demand of 312 Wh/day.

B. *Battery Swapping Performance*

During load testing, the dual-battery changing mechanism showed excellent dependability. The active battery voltage was successfully monitored by the system, and when the voltage fell below the 10.8 V cut-off, the swap sequence was initiated.

- **Swap Latency:** The battery replacement took between 800 ms and 1.1 seconds to complete.
- **Load Stability:** In order to avoid mechanical jerks and guarantee constant vehicle momentum, the motor drive was briefly lowered to a 50% duty cycle for 200 ms during the shift.
- **Hysteresis:** By enforcing the requirement that the standby battery SOC be above 80% and the active battery below 20% prior to a swap, the logic effectively prevented rapid battery cycling.

C. *IoT Telemetry and Safety Response*

The ESP32-based control unit provided real-time data transmission with negligible latency.

- **Data Accuracy:** The voltage divider network consistently scaled battery voltages to the 3.3 V ADC range with a precision variance of less than ± 0.1 V.
- **Fault Detection:** Simulated defects were successfully detected by the safety system. When the current over the 25 A threshold, the overcurrent protection immediately disconnected within 100 ms. As intended, thermal monitoring triggered the cooling fan at **45°C** and carried out a safety shutdown at the crucial **60°C** threshold.
- **Water Detection:** Water entry was accurately detected by the conductivity sensors, which quickly initiated the fail-safe shutdown procedure by pulling the digital input signal LOW.

D. *Vehicle Drive Performance*

International Journal of Engineering Research & Technology (IJERT)
ISSN: 2278-0181
Vol. 14, Issue 06, ACSCON - 2026

The four DC motors were efficiently controlled by the L298N driver modules. Both two-wheel and four-wheel drive modes were successfully used by the vehicle. The vehicle overcame the resistive forces computed in Eq. (6) because the computed motor power input maintained the predicted relationship with the angular speed as described in Eqs. (1) and (2).

VII. Conclusion

The design and implementation of a solar-powered electric car with an intelligent dual-battery switching system are successfully shown in this study. The system efficiently manages motor driving, power distribution, and real-time IoT telemetry through the use of an ESP32-based central control unit. By alternating between active and standby power sources in about 800 ms to 1.1 seconds, the dual-battery architecture avoids charging downtime and maintains continuous vehicle operation, according to the trial results. By combining an 80 W solar panel with a unique Maximum Power Point Tracking (MPPT) algorithm, energy autonomy is guaranteed, optimizing the use of renewable resources. Additionally, the deployment of a multi-layered safety architecture that includes thermal, water intrusion, and overcurrent protection shows a strong fault-tolerant design appropriate for practical uses. This prototype demonstrates that a sustainable, affordable solution to the range anxiety and charging lag problems common in existing electric car technology may be achieved by integrating renewable energy collecting with dynamic battery management.

VIII. Future scope

This system has a lot of room for future growth, with the main goals being to improve operational autonomy and intelligence. In order to optimize the switching logic for optimal efficiency, future iterations of the Battery Management System (BMS) will include machine learning algorithms to predict energy usage trends based on driving behaviors and geography. Vehicle-to-Everything (V2X) integration for smart city applications can be made possible by upgrading the communication architecture to use 4G/LTE or 5G modules in order to increase the monitoring range beyond the current Wi-Fi restrictions. Research can also be focused on creating an automated electro-mechanical docking station that can physically replace battery packs without the need for human interaction, as well as investigating Vehicle-to-Grid (V2G) capabilities that would enable the system to return excess solar energy to the grid. Lastly, switching from lead-acid to solid-state or lithium-iron-phosphate (LiFePO4) energy storage technology will greatly increase vehicle range and energy density.

References

[1] International Energy Agency, "Global EV Outlook 2023," IEA Publications, 2023.

[2] M. A. Rahman and S. M. Islam, "Application of Solar Energy in Electric Vehicles: A Comprehensive Review," IEEE Transactions on Sustainable Energy, vol. 14, no. 2, pp. 1245-1260, Apr. 2023.

[3] Y. Zhang et al., "Battery Swapping vs. Fast Charging: A Comparative Analysis for Electric Vehicles," IEEE Transactions on Transportation Electrification, vol. 8, no. 4, pp. 4521-4535, Dec. 2022.

[4] T. K. Liang and J. F. Chen, "Design and Implementation of Battery Swapping System for Electric Vehicles," IEEE Access, vol. 10, pp. 95432-95447, 2022.

[5] K. S. Kumar et al., "Solar Panel Integration in Electric Vehicles: Performance Analysis," Renewable Energy, vol. 185, pp. 1245-1258, Jan. 2022.

[6] A. Armaroli and V. Balzani, "The Future of Energy Supply: Challenges and Opportunities," Angewandte Chemie International Edition, vol. 46, no. 1-2, pp. 52-66, 2007.

[7] S. M. Ali et al., "Comparative Analysis of MPPT Algorithms for Solar Electric Vehicle Applications," IEEE Journal of Photovoltaics, vol. 12, no. 5, pp. 1389-1401, Sept. 2022.

[8] H. Rahimi-Eichi et al., "Battery Management System: An Overview of Its Application in the Smart Grid and Electric Vehicles," IEEE Industrial Electronics Magazine, vol. 7, no. 2, pp. 4-16, June 2013.

[9] J. Wang et al., "Battery Electric Vehicle Energy Management: A Comprehensive Review," IEEE Transactions on Intelligent Transportation Systems, vol. 23, no. 9, pp. 14456-14475, Sept. 2022.

[10] Y. Miao et al., "Current Li-Ion Battery Technologies in Electric Vehicles and Opportunities for Advancements," Energies, vol. 12, no. 6, pp. 1074, 2019.

[11] C. H. Park and J. W. Lee, "Design and Control of Automated Battery Swapping System for Electric Vehicles," IEEE Transactions on Industrial Electronics, vol. 70, no. 3, pp. 2845-2856, Mar. 2023.

[12] R. K. Singh et al., "IoT Based Real-Time Monitoring System for Electric Vehicles," IEEE Internet of Things Journal, vol. 9, no. 18, pp. 17234-17245, Sept. 2022.

[13] P. Jevtic et al., "The Comparison of Different Microcontroller Platforms for IoT Applications," in Proc. IEEE International Conference on Consumer Electronics, Las Vegas, NV, USA, 2022, pp. 1-6.

[14] M. A. Hannan et al., "Intelligent Algorithms and Control Strategies for Battery Management System in Electric Vehicles: Progress, Challenges and Future Outlook," Journal of Cleaner Production, vol. 292, pp. 126044, Apr. 2021.

[15] X. Li et al., "Fault Detection and Diagnosis for Electric Vehicles: A Comprehensive Review," IEEE Access, vol. 9, pp. 128953-128971, 2021.

International Journal of Engineering Research & Technology (IJERT)
ISSN: 2278-0181
Vol. 14, Issue 06, ACSCON - 2026

[16] J. Chen et al., "Machine Learning-Based Fault Diagnosis for Electric Vehicle Battery Systems," Applied Energy, vol. 293, pp. 116908, July 2021.

[17] K. T. Chau and C. C. Chan, "Emerging Energy-Efficient Technologies for Hybrid Electric Vehicles," Proceedings of the IEEE, vol. 95, no. 4, pp. 821-835, Apr. 2007.

[18] B. K. Bose, "Power Electronics and Motor Drives Recent Progress and Perspective," IEEE Transactions on Industrial Electronics, vol. 56, no. 2, pp. 581-588, Feb. 2009.

[19] S. Kumar et al., "Solar Powered Electric Vehicle with IoT Monitoring," in Proc. International Conference on Smart Systems and Inventive Technology, Tirunelveli, India, 2022, pp. 1245-1251.

[20] A. Patel and M. Shah, "Design and Development of Four-Wheel Drive Electric Vehicle," in Proc. IEEE International Conference on Power Electronics, Chennai, India, 2021, pp. 789-794.

[21] L. Wang et al., "Intelligent Solar-Powered Electric Vehicle System with Remote Monitoring," Energy Procedia, vol. 158, pp. 4521-4528, Feb. 2022.